Enhancement of photoluminescence intensity by photoinduced interdiffusion in nanolayered *a*-Se/As_2S_3 films

K. V. Adarsh and K. S. Sangunni[a)]
Department of Physics, Indian Institute of Science, Bangalore, 560012 India

S. Kokenyesi and I. Ivan
Department of Experimental Physics, University of Debrecen, Bem ter 18/a, Debrecen, 4026 Hungary

M. Shipljak
Uzhgorod National University, Pidhirna 46, Uzhgorod, 88000 Ukraine

(Received 4 August 2004; accepted 1 December 2004; published online 26 January 2005)

Optical parameters of chalcogenide glass multilayers with 12–15 nm modulation lengths prepared by thermal evaporation can be changed by laser irradiation. Photoluminescence (PL) studies were carried out on such nonirradiated and irradiated multilayered samples of *a*-Se/As_2S_3 (sublayer thickness of *a*-Se is 4–5 nm for one set of samples and 1–2 nm for the other set. However As_2S_3 sublayer thickness is 11–12 nm for both sets of samples.) PL intensity can be increased by several orders of magnitude by reducing the Se well layer (lower band gap) thickness and can be further increased by irradiating the samples with appropriate wavelengths in the range of the absorption edge. The broadening of luminescence bands takes place either with a decrease in Se layer thickness or with irradiation. The former is due to the change in interface roughness and defects because of the enhanced structural disorder while the latter is due to photoinduced interdiffusion. The photoinduced interdiffusion creates defects at the interface between Se and As_2S_3 by forming an As–Se–S solid solution. From the deconvoluted PL spectrum, it is shown that the peak PL intensity, full width half maximum, and the PL quantum efficiency of particular defects giving rise to PL, can be tuned by changing the sublayer thickness or by interdiffusion. © *2005 American Institute of Physics*. [DOI: 10.1063/1.1853499]

INTRODUCTION

Availability of amorphous semiconductors in the form of high quality multilayers provide potential applications in the field of micro- and optoelectronics.[1,2] Although the misfit problems in amorphous multilayers (AMLs) are considerably reduced compared to crystalline superlattices, there are still some physical processes (e.g., quantum confinement, diffusion) that are not well understood.[3–5]

Among AMLs, chalcogenide multilayers are attractive because of the prominent photoinduced effects. Studies in chalcogenide AML have been directed towards two phenomena. One of them is photoinduced diffusion in short period multilayer systems, which finds potential applications in holographic recording and fabrication of phase gratings.[2,6] The other is photodarkening or bleaching,[4,7–10] which is also known in thick films.[8,11] Studies on nanostructured chalcogenides are still in the infant stage.

Luminescence properties of group IV AMLs (like *a*-Si:H/*a*-$Si_{0.8}N_{0.2}$)[1] as well as homogeneous thin films of chalcogens like Se, As_2S_3, As_2Se_3 are widely studied.[12–14] On the other hand, there are no reports about the luminescence of chalcogenide AMLs. The Mott Davis street (MDS) model or charged dangling bond model[15,16] for chalcogenide glass states that the luminescence does indeed occur at defects but the associated states in the gap lie near to one or the other of the band. This model satisfactory explains the continuous wave photoluminescence (PL), which accounts for most of the PL quantum efficiency. A photoinduced electron (e^-) or hole (h^+) is trapped by an isolated charged defect

$$D^+ + e^- \rightarrow D^0, \quad D^- + h^+ \rightarrow D^0$$

and then a hole or electron recombines with the D^0:

$$D^0 + e^- \rightarrow D^- + h\upsilon_{\mathrm{PL}}, \quad D^0 + h^+ \rightarrow D^+ + h\upsilon_{\mathrm{PL}},$$

where h is the Plank constant, υ_{PL} is the frequency of the emitted radiation, D stands for the chalogen dangling bond, and the superscripts stand for the charge state. In the valence alternation pair (VAP)[17] model D^+, D^- are identified as C_3^+ and C_1^- where C stands for chalcogen atom and subscripts and superscripts stand for coordination number and charge state, respectively. If C_3^+ and C_1^- are formed very close to each other, they are termed as the intimate valence alternation pair (IVAP). But the time resolved PL experiments[18,19] showed that the PL decay can be divided into two regimes, one of which is dominated by the process characterized by short times ($t \leqslant 10^{-6}$ s) and the other by longer times ($t \geqslant 10^{-4}$ s); the long time process accounts for most of the PL quantum efficiency and therefore they dominate the steady state behavior. The MDS model could not explain these short and long time decay processes. Higashi and Kastner[19] suggested that the long time decay process is the result of triplet recombination at IVAPs and the short time decay process is the result of singlet recombination at the isolated VAPs. Both VAPs and IVAPs take part in luminescence. Recently PL

[a)]Author to whom correspondence should be addressed; electronic mail: sangu@physics.iisc.ernet.in

lifetime measured by quadrature frequency resolved spectroscopy[20] showed double peak lifetime distributions in As_2S_3 and Se that are very similar to that observed in *a*-Si:H and *a*-Ge:H.[21] The double peak lifetime distribution in *a*-Si:H and *a*-Ge:H is explained by an exciton model[21] in which the short time component is due to the radiative recombination of singlet excitons and the long lived component is due to triplet excitons. A self-trapped exciton model reasonably explains the two component lifetime and PL stoke shift in amorphous chalcogenides,[20] with the short lived and long lived components attributed to singlet and triplet excitons, respectively, where the excitons can be created from specific bonds. In this article we report the PL from *a*-Se/As_2S_3 MLs. Earlier reports showed that there is an increase in the band gap up to 0.05 eV in as-prepared chalcogenide AMLs in comparison with thick films and an additional increase is caused by heat treatment or light irradiation.[4,22,23] Increase in the band gap of the irradiated films is assumed to occur because of the intermixing of adjacent sublayers due to interdiffusion. We irradiated the earlier samples and took the PL to understand the changes of defects and energy spectrum of the compositionally modulated nanostructures.

EXPERIMENTAL PROCEDURES

The *a*-Se/As_2S_3-type ML1 (sublayer thickness of *a*-Se and As_2S_3 are 4–5 and 11–12 nm) and ML2 (*a*-Se 1–2 nm, As_2S_3 11–12 nm) were prepared by cyclic thermal evaporation technique from bulk (powered) *a*-Se and As_2S_3. The deposition rates were 2–10 nm/s in vacuum with a basic pressure of 5×10^{-4} Pa. Periodicity was monitored by the low angle x-ray diffraction method.[2] To study photostimulated effects we irradiated the as-prepared samples with a diode pumped solid state laser of wavelength 532 nm and a power density of 1 W/cm^2 up to 40 min at room temperature. Some of the samples were irradiated with a He–Ne laser ($\lambda=633$ nm, power density 0.8 W/cm^2) at the same temperature and optical absorption measurements were carried out. The objective is to check the band gap of *a*-Se or $Se_x(As_2S_3)_{1-x}$ solid solutions since these mostly determine the absorption of the as-deposited or treated AML, where As_2S_3 is a wide band gap barrier. These measurements were carried out on a HP-8453-type spectrophotometer at room temperatures.

PL studies were carried out on "as-prepared" and irradiated samples at 4.2 K by using a Fourier-transform spectrometer (MIDAC Corp., USA). An Ar^+ laser ($\lambda=514.5$ nm) of 2 mm beam divergence with a power density of 100 mW/cm^2 was used for luminescence excitation. Samples were mounted on a sample holder that had the provision to mount 20 samples at a time and were then suspended in a liquid He cryostat attached to the spectrometer. The PL signals from the samples were analyzed by using a Michelson interferometer and were detected by using a liquid nitrogen cooled Ge photodiode. The interferograms spanning the entire 0.6–1.8 eV range were recorded by taking an average of over ten scans for nearly 30 s using a personal computer attached to the spectrometer. The excitation was turned on just before recording each spectrum to avoid luminescence fatigue. CdTe, which has fine luminescence, features in the 1.35–1.4 eV range[24] was used for calibration.

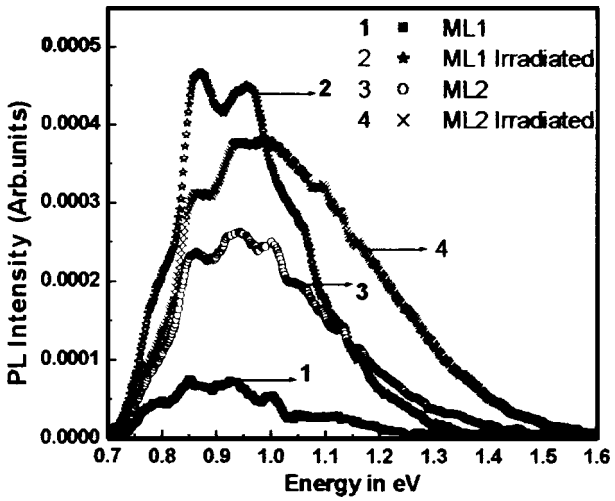

FIG. 1. Experimental PL spectra of as-prepared and irradiated multilayered samples at 4.2 K. As-prepared samples were irradiated with a diode pumped solid state laser of wavelength 532 nm and a power density of 1 W/cm^2 up to 40 min at room temperature to produce photoinduced interdiffusion between the multilayers.

RESULTS AND DISCUSSIONS

None of the AML samples showed PL at 77 K, which clearly indicate that there exists a competitive nonradiative mechanism, similar to the separate homogeneous *a*-Se or As_2S_3 layers. PL spectra of as-prepared and irradiated samples at 4.2 K are given in Fig. 1. In our samples we kept the number of Se and As_2S_3 layers constant where as the Se layer thickness varied and As_2S_3 layer thickness was maintained constant. We observed a broad PL in the range of 0.8–1.2 eV. Since the PL was well below the band gap with different peaks of varying intensity, we could not get the information about the band gap or the blueshift of luminescence. The situation is more simple for near band gap luminescence in Se nanocrystals embedded into the polymer host,[25] which shows a blueshift of the luminescence peak up to 0.23 eV in 4.3 nm size nanoparticles. A blueshift of the absorption edge with a decrease in thickness of the absorption amorphous semiconductor layer was observed in different AMLs.[1–4] A blueshift of the optical absorption edge $\Delta E_g^* \approx 0.05$ eV was observed in our as prepared multilayered samples and can be increased further by irradiation (Fig. 2). An additional increase in the measured band gap by irradiation is due to the intermixing of well layers of Se and barrier layers of As_2S_3 to form the solid solution of $(As_2S_3)_{1-x}Se_x$.[6,22] There is not much change in the peak PL energy values of the irradiated samples over the as-prepared samples whereas the PL intensities of irradiated samples are greater than that of the as-prepared samples.

Irradiation at room temperature produces two types of effects. One is the photoinduced interdiffusion and the other is the defect creation. Illumination at room temperature can produce the IVAPs and VAPs[26] like $As_4^+-S_1^-$, $As_2^+-S_1^-$, Se_3^+, and Se_1^-. These defects can act as luminescence centers. In-

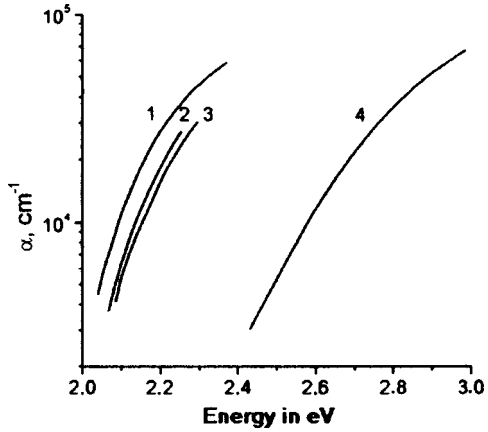

FIG. 2. Optical absorption edges of homogeneous 1-μm-thick *a*-Se (1) As_2S_3 (4) and the same for as prepared (2) and irradiated (3) Se/As_2S_3 multilayered samples.

terdiffusion between the layers, which can also produce more luminescencet centers, i.e., the interdiffusion of As_2S_3 and Se layers will create positively and negatively charged dangling bonds (IVAPs and VAPs) by breaking the Se chains or As_2S_3 polyhedron in the mixed region. The earlier assumption is based on the fact that we can increase the PL intensity of *a*-Se by doping with Ge or As.[15,27] Here the fourfold and threefold cocoordinated Ge and As will break the long Se chains creating the VAPs and IVAPs that are the native centers of PL. These two effects play an important role in the increase in PL of irradiated samples over the as prepared samples. PL intensity of irradiated ML1 (I-ML1) is greater than that of the irradiated ML2 (I-ML2). This can be understood by comparing the change in PL intensity of irradiated and as-prepared samples of both sets. PL intensity of I-ML1 is five times greater than that of the as prepared ML1, whereas the PL intensity of I-ML2 is one and a half times greater than that of the as prepared ML2. This shows that ML2 is not as sensitive to irradiation as compared to ML1, more precisely stimulated changes are smaller because of the thin Se layers (holographic efficiency which is at the expense of interdiffusion between the sublayers showed that the optimum thickness of Se layer in MLs are 4–6 nm[6]).

The width of the PL increases with decrease in Se sublayer thickness (Fig. 1). The increase in width may be due to the change in roughness of the interface, since the final state of the very thin Se layer before the complete interdiffusion probably looks like islands in the As–S–Se matrix. A decrease in Se sublayer thickness results in a small increased structural disorder connected with a possible bond angle distribution change,[6] similar to that of *a*-Si:H/*a*-SiN_x superlattices.[28] The observed increase in the luminescence width in our system is similar to that of the change in PL width with interface roughness of quantum well heterostructures[29] (QWH) where the broadening is due to the island like structures and is explained quantitatively by using line shape theory. An important feature of this elementary theory is the tendency for the PL line to exhibit an infinitely increasing linewidth when the thickness of the well layers decreases to low values. The same type of increase in the linewidth is observed in our multilayered system with the

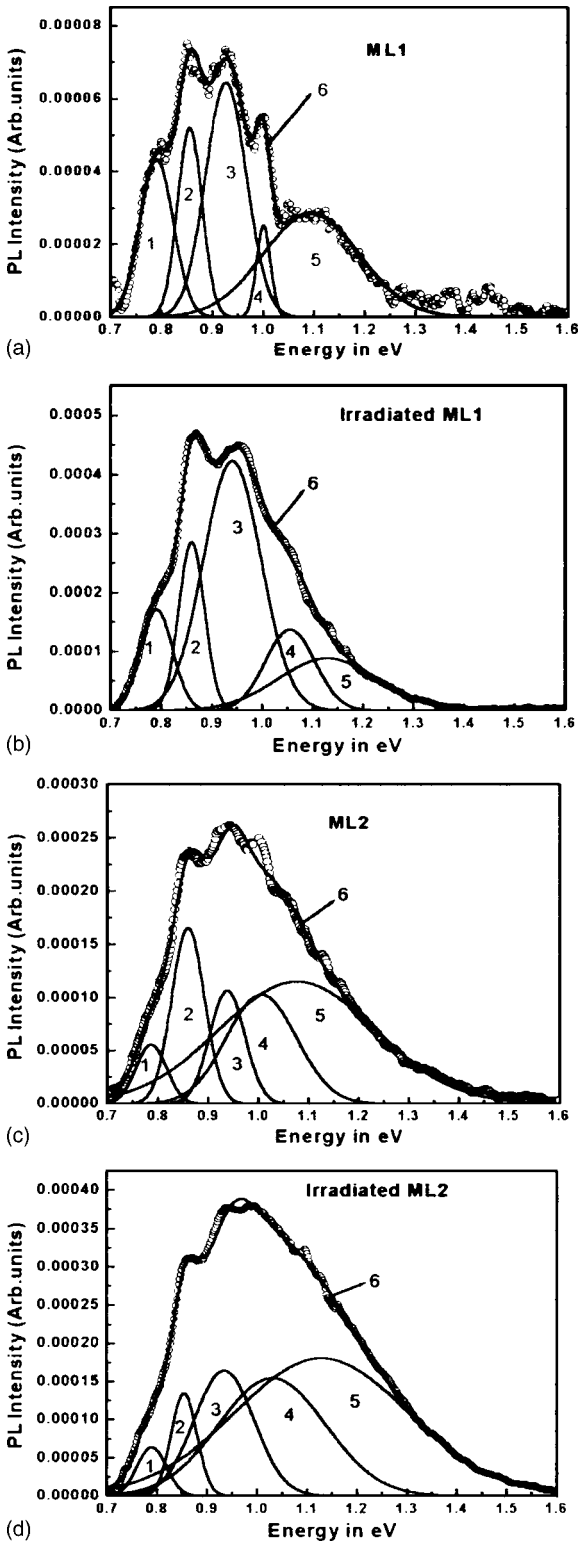

FIG. 3. Deconvoluted experimental PL spectra of (a) ML1, (b) I-ML1, (c) ML2, and (d) I-ML2. The experimental spectra are represented by symbols "○;" deconvoluted spectra are represented by curves 1,2,3,4,5. The resultant of the deconvoluted spectra is represented by curve 6.

decrease in the Se well layer thickness. The situation is the same under illumination also. The increase in the PL width of the irradiated samples over the as-prepared samples shows the level of structural disorder at the interface. This clearly indicates the decrease of Se layer thickness due to the interdiffusion and solid solution formation at the $Se-As_2S_3$ inter-

TABLE I. The PL peak energy of different transitions extracted from the deconvoluted spectra of as-prepared and irradiated samples.

Sample	Peak 1 (eV)	Peak 2 (eV)	Peak 3 (eV)	Peak 4 (eV)	Peak 5 (eV)
ML1	0.79	0.86	0.93	1	1.09
I-ML1	0.79	0.86	0.94	1.06	1.13
ML2	0.79	0.86	0.94	1	1.08
I-ML2	0.79	0.86	0.94	1.03	1.12

faces, which is accompanied by the tail state broadening and creation of additional defects. The two competitive effects of (a) band gap broadening in AML due to a decrease in Se thickness and As–S–Se solid solution formation (b) band tail broadening, additional defect creation, make the PL data analysis rather complex.

Luminescent transitions at low temperatures are generally described by a Gaussian line broadening mechanism and can be written as[15]

$$I(h\nu) \propto \exp[-(h\nu - E^* + 2W)^2/\sigma^2], \tag{1}$$

where E^* is the energy separation between the excited state and zero phonon energy ($q=0$) of the ground state, $2W$ is the Stoke shift, and σ is the standard deviation. Many experiments on QWH prove that a deconvolution of the measured luminescence line shapes provides quantitative otherwise inaccessible information on structural and the chemical properties of the interface in the QWH. Since our luminescence spectrum contains more than one Gaussian peak, we deconvoluted the spectrum to obtain more information about the luminescence centers. The Levenberg–Marquardt "chi^2" minimizing algorithm[30,31] was used to deconvolute each experimental spectrum into a combination of Gaussians given by

$$I(h\nu) = I(0) + \sum_{i=1}^{i=n} A_i \exp\left\{-2\left[\frac{(x - xc_i)^2}{w_i^2}\right]\right\}, \tag{2}$$

where $I(0)$ represents the offset, A_i, xc_i, $2.355w_i$ representing amplitude, peak position, and full width half maxima of the ith transition, respectively. The deconvoluted spectra of as-prepared and irradiated samples show five peaks (Fig. 3). The extracted features from the deconvoluted spectra are given in the Tables I–IV.

The PL peak energy of all the transitions obtained by deconvoluting the experimental data is given in the Table I. The first two peaks of irradiated and as-prepared samples are at the same position. The third peak is at 0.94 eV for all the samples except for ML1 where it is at 0.93 eV. The fourth and fifth peaks of the irradiated samples are shifting to higher energies compared to the as-prepared samples. This may be because of the intermixing of the Se and As_2S_3 layer. The peak PL intensities of the deconvoluted peaks of as-prepared and irradiated samples are given in Table IV. The PL intensity shows its maximum for the third peak in the case of ML1, but for ML2 it is the second peak. The increase in PL intensity of the second peak of ML2 over ML1 may be because of the more disordered Se interface, which has an emission at 0.86 eV.[27] But for I-ML1 and I-ML2 the maximum intense peaks are third and fifth, respectively. This may be due to the extent of interdiffusion.

TABLE III. Area under the curve (photoluminescence quantum efficiency) of respective transitions extracted from the deconvoluted spectra of as-prepared and irradiated samples. Area= $\sqrt{2\pi}A_i\sigma_i$ where A_i and σ_i are amplitude and full width at half maximum of the respective transitions. All the values are scaled by a factor of 1×10^{-5}.

Sample	Peak 1	Peak 2	Peak 3	Peak 4	Peak 5
ML1	0.36	0.31	0.65	0.09	0.68
I-ML1	1	2	6	2	2
ML2	0.43	1	0.94	2	5
I-ML2	0.47	0.87	2	4	8

The integrated area under the peak will give the photoluminescence quantum efficiency (PLQ).[12] Variations of the PLQ of different peaks of the as-prepared and irradiated samples are given in Table III. The third peak of ML1 and I-ML1 and the fifth peak of ML2 and I-Ml2 show the maximum PLQ. The reason for the change may be due to the decrease in a-Se thickness. The full width at half maximum (FWHM) also shows a similar trend and is given in Table II. FWHM of the first two peaks is the same for the irradiated and as-prepared samples.

The PL of the homogeneous As_2S_3 layer of thickness 3.3 μm shows five peaks after deconvolution and they are at 0.79, 0.85, 0.92, 1, and 1.1 (all in eVs). But the a-Se thin film of thickness comparable to the total sublayer thickness of a-Se in the multilayer has showed no luminescence. This may be because the thickness is not sufficient to give a detectable PL intensity or the luminescence from a-Se[32] is very weak. Deconvoluted spectrum of bulk a-Se showed three peaks and they are at 0.85, 0.86, and 0.95 (all in eVs).[27] By comparing the PL peak energy values of AMLs with homogeneous a-Se and As_2S_3 it is clear that the luminescence is from both Se and As_2S_3. The fourth peak at 1.03 eV in the case of I-ML2 and 1.06 eV in the case of I-ML1 may be because of the $Se_x(As_2S_3)_{1-x}$ solid solution formation since

TABLE II. Full width at half maximum of different transitions extracted from the deconvoluted spectra of as-prepared and irradiated samples.

Sample	Peak 1 (eV)	Peak 2 (eV)	Peak 3 (eV)	Peak 4 (eV)	Peak 5 (eV)
ML1	0.06	0.05	0.08	0.03	0.19
I-ML1	0.06	0.05	0.11	0.1	0.19
ML2	0.06	0.05	0.07	0.14	0.31
I-ML2	0.06	0.05	0.12	0.21	0.35

TABLE IV. The peak PL intensity of different transitions extracted from the deconvoluted spectra of as-prepared and irradiated samples. All the values are scaled by a factor of 1×10^{-4}.

Sample	Peak 1	Peak 2	Peak 3	Peak 4	Peak 5
ML1	0.29	0.25	0.64	0.52	0.43
I-ML1	1.72	2.86	4.23	1.38	0.89
ML2	0.56	1.65	1.04	1.01	1.15
I-ML2	0.64	1.33	1.65	1.55	1.81

the PL of $Se_x(As_2S_3)_{1-x}$ is around this energy.[15] The increase in the energy of the fifth peak of irradiated MLs over the as-prepared MLs may be due to the decrease in the As_2S_3 sublayer by interdiffusion. The PL at 1.1 eV is mainly from the As–S bond.[26,33]

All these results indicate the high impact of interdiffusion on the luminescence intensity in the given AML is due to changes of defect states, which in turn are not directly connected to the band structure, i.e., confinement effects are not essential for this type of luminescence. The role and influence of the possible stress in the AML on luminescence can be expected but it is hard to determine the same through such experiments.

CONCLUSION

It is shown that reducing the thickness of the Se well layer can increase the PL efficiency of the multilayer, which can be further increased by irradiation. It is also shown that the broadening of the PL line shape is due to the change in interface roughness, which is well known in the QWH. Deconvolution showed that the PL spectrum consists of five transitions. The deconvoluted peak PL intensity, PLQ and FWHM are varying according to the function of sublayer thickness and interdiffusion. The whole picture is complex due to more complicated carrier relaxation and recombination process, possibly with several interconnected effects, which are not properly understood, but the possibility for tuning the optical parameters of the AML, including the low temperature luminescence, is established.

ACKNOWLEDGMENTS

K.V.A. thanks CSIR for financial support. The authors thank Dr. K. S. R. K. Rao and Naresh Babu for PL measurements, as well as the support of bilateral Indo-Ukrainian R&D and Hungarian OTKA (N T046758) grants.

[1] M. Hirose and S. Miyazaki, Japan Annual Reviews in Electronics, Computers and Telecommunications **22**, 147 (1987).
[2] V. Palyok, A. Mishak, I. Szabo, D. L. Beke, and A. Kikineshi, Appl. Phys. A: Mater. Sci. Process. **68**, 489 (1999).
[3] D. Nesheva, D. Arsova, and Z. Levi, Philos. Mag. B **69**, 205 (1994).
[4] A. Kikineshi and A. Mishak, NATO ASI Ser., Ser. E **36**, 249 (1997).
[5] A. L. Greer, Defect Diffus. Forum **129–130**, 163 (1996).
[6] T. Wagner and P. J. S. Ewen, J. Non-Cryst. Solids **266–269**, 979 (2000).
[7] A. Kikineshi, Opt. Eng. **34**, 1040 (1995).
[8] H. Eguchi, Y. Suzuki, and M. Hirai, J. Non-Cryst. Solids **95–96**, 757 (1987).
[9] K. Hayashi and N. Mitsuishi, J. Non-Cryst. Solids **299–302**, 949 (2002).
[10] K. Tanaka, S. Kyohya, and A. Odajima, Thin Solid Films **111**, 195 (1984).
[11] I. I. Turjanitsa, A. Kikineshi, and D. G., Ukr. Phys. J. **24**, 534 (1979).
[12] T. Tiedje, B. Abeles, and B. G. Brooks, Phys. Rev. Lett. **54**, 2545 (1985).
[13] Y. Kanemitsu and T. Kushida, Appl. Phys. Lett. **77**, 3550 (2000).
[14] G. Pucker, P. Belluti, C. Spinella, K. Gatterer, M. Cazzanelli, and L. Pavesi, J. Appl. Phys. **88**, 6044 (2000).
[15] R. A. Street, Adv. Phys. **25**, 397 (1976).
[16] R. A. Street and N. F. Mott, Phys. Rev. Lett. **35**, 1293 (1975).
[17] M. Kastner, D. Adler, and H. Fritzsche, Phys. Rev. Lett. **37**, 1504 (1976).
[18] K. Murayama, J. Non-Cryst. Solids **59–60**, 983 (1983).
[19] G. S. Higashi and M. A. Kastner, Philos. Mag. B **47**, 83 (1983).
[20] T. Aoki, S. Komedoori, S. Kobayashi, T. Shimizu, A. Ganjoo, and K. Shimkawa, J. Non-Cryst. Solids **326–327**, 273 (2003).
[21] R. Stachowitz, M. Schubert, and W. Fuhs, J. Non-Cryst. Solids **227–230**, 190 (1998).
[22] A. Csik, M. Malyovanik, J. Dorogovics, A. Kikineshi, D. L. Beke, I. A. Szabo, and G. Langer, J. Optoelectron. Adv. Mater. **3**, 33 (2001).
[23] M. Malyovanik, M. Shiplyak, V. Cheresnya, T. Remeta, S. Ivan, and A. Kikineshi, J. Optoelectron. Adv. Mater. **5**, 397 (2003).
[24] G. Suma, H. L. Bhat, B. Sunderseshu, R. K. Bagai, and V. Kumar, Appl. Phys. Lett. **68**, 2424 (1996).
[25] M. Rajalakshmi and A. K. Arora, Solid State Commun. **110**, 75 (1999).
[26] K. Shimakawa, A. V. Kolobov, and S. R. Elliot, Adv. Phys. **44**, 475 (1995).
[27] N. Asha Bhat, K. S. Sangunni, and K. S. R. K. Rao, J. Non-Cryst. Solids **319**, 192 (2003).
[28] N. Maley and J. S. Lanin, Phys. Rev. B **31**, 5577 (1985).
[29] M. A. Herman, D. Bimberg, and J. Christen, J. Appl. Phys. **70**, R1 (1991).
[30] J. J. More, in *Numerical Analysis*, Lecture Notes in Mathematics 630, edited by G. A. Watson (Springer, New York, 1977), pp. 105–116.
[31] P. R. Bevington, *Data Reduction and Error Analysis for the Physical Sciences*, (McGraw-Hill, New York, 1969).
[32] R. A. Street, Philos. Mag. **30**, 1181 (1974).
[33] T. Tada and T. Ninomaya, J. Non-Cryst. Solids **114**, 88 (1989).